

## Oscillatory driven colloidal binary mixtures: Axial segregation versus laning

Adam Wysocki and Hartmut Löwen

*Institut für Theoretische Physik II: Weiche Materie, Heinrich-Heine-Universität Düsseldorf,**Universitätsstraße 1, D-40225 Düsseldorf, Germany*

(Received 21 January 2009; published 28 April 2009)

Using Brownian dynamics computer simulations we show that binary mixtures of colloids driven in opposite directions by an oscillating external field exhibit axial segregation in sheets perpendicular to the drive direction. The segregation effect is stable only in a finite window of oscillation frequencies and driving strengths and is taken over by lane formation in the direction of the driving field if the driving force is increased or the oscillation frequency is decreased. In the crossover regime, bands tilted relative to the drive direction are observed. Possible experiments to verify the axial segregation are discussed.

DOI: 10.1103/PhysRevE.79.041408

PACS number(s): 82.70.Dd, 61.20.Ja

Phase transitions in driven systems are qualitatively different from their equilibrium counterparts and reveal a wealth of novel instabilities and pattern formations induced by nonequilibrium conditions [1]. In particular, it is very intriguing to resolve and follow nonequilibrium dynamics on the particle level which is possible for granular grains [2,3], mesoscopic colloidal suspensions [4], or dusty plasmas driven by an external field [5].

In the colloidal context, recent investigations have focused on binary mixtures which are driven by a constant but species-dependent force. The latter can be realized by gravity [6,7] or by an electric field [8]. If the drive is strong enough, lanes of particles driven alike are formed in the direction of the driving field [9].

In this paper we simulate a model for a colloidal mixture with a time-dependent oscillatory drive [10]. We show that this induces an axial segregation, i.e., an ordering in sheets normal to the driving field (rather than parallel as for laning). While such an axial segregation of two-particle species is observed in shaken or vibrated granular systems [11–14], it has not yet been described for colloidal suspensions whose dynamics is dominated by overdamped Brownian motion. This makes the colloidal dynamics different from that of granular systems where inelastic collisions play an important role. At fixed density, we map out the whole nonequilibrium steady-state diagram over a large range of frequencies and driving amplitudes and find a rich phase diagram topology. By increasing the magnitude of the driving force or decreasing the oscillation frequency, the system gets back either to a disordered state or to lane formation with an intermediate regime where mixing of segregation and tilted lanes occurs. Decreasing the magnitude of the driving or increasing the oscillation frequency, on the other hand, always yields a disordered steady state. We then study the relaxational dynamics into the steady states and show that first laning occurs and if at all axial segregation occurs on a larger time scale. Finally we discuss the anisotropy of the mean-square displacements (MSDs) in the different steady states as dynamical consequences of their different structure.

In order to simulate the dynamics of a colloidal suspension we utilize a two-dimensional Brownian dynamics (BD) simulation with neglected hydrodynamic interactions between the particles. In particular, we consider an equimolar binary mixture of  $N=2864$  hard disks of diameter  $\sigma$  [15].

In Brownian dynamics, the time evolution of the individual colloids is governed by overdamped Langevin equation with thermal noise [16,17]. The particles of sort  $A$  and  $B$  are subjected to an oscillatory inversely phased force  $\mathbf{f}^A(t)=-\mathbf{f}^B(t)=f_0 \sin(\omega t)\mathbf{e}_x$ , where  $\omega$  is the driving frequency and  $f_0$  is the driving strength. A single particle will follow a noise-averaged trajectory which is sinusoidal in time with an amplitude  $f_0/(\xi\omega)$ , where  $\xi$  is the friction constant.

We simulate a quadratic system of size  $L/\sigma=75$  with periodic boundary conditions at a total area fraction  $\phi=N\pi\sigma^2/(4L^2)=0.4$  [18]. As a measure for the driving strength, we define the Peclet number  $Pe=\tau_D/\tau_d$  as the ratio between the time  $\tau_D=\sigma^2/(4D)$  it takes a colloid to diffuse its own radius and the time  $\tau_d=\sigma/(2v_d)$  it takes to drift the same distance under the action of a constant external force  $f_0$ . Here  $D=k_B T/\xi$  denotes the short-time diffusion constant, where  $k_B T$  is the thermal energy and  $v_d=f_0/\xi$  is the maximal drift velocity.

The initial configuration of the BD simulation is an equilibrated fully mixed configuration as realized in the absence of the drive. At time  $t=0$ , the oscillatory force is turned on instantaneously and the evolution of the system is followed by using a finite time-step algorithm [16,17] up to about  $10^5$  oscillation periods. Depending on the Peclet number  $Pe$  and the reduced frequency  $\omega\tau_D$ , the system ends up in different steady states.

The nonequilibrium steady-state phase diagram is shown in Fig. 1 spanning two decades in both driving frequency  $\omega\tau_D$  and strength  $Pe$ . For the corresponding movie showing the development from the initial to the steady state, see [19]. Let us discuss the topology of the phase diagram step by step. For very low driving strengths, the external drive is not strong enough to generate order in the completely mixed equilibrium state leading to a *disordered* steady state which is depicted in a typical snapshot in Fig. 1(a). A disordered state is rendered as crosses in the full phase diagram shown in Fig. 1(e) such that the region of low Peclet numbers involves a disordered steady state. As visible in Fig. 1(a), the disordered state can possess an intrinsic finite correlation length as set by colliding clusters which is larger than the interparticle distance but these structures do not span the whole simulation box. For very high frequencies, on the other hand, a free particle would just perform oscillations with a very small amplitude due to the drive. This amplitude

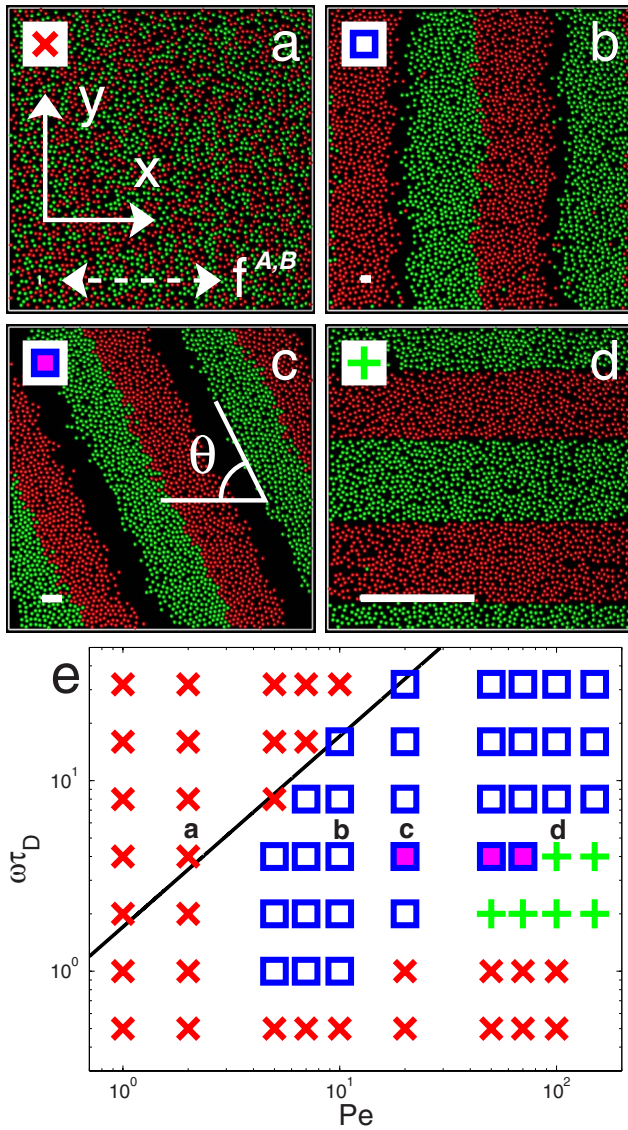


FIG. 1. (Color online) [(a)–(d)] BD simulation snapshots for fixed driving frequency  $\omega\tau_D=4$  but different Peclet numbers  $Pe$  after  $10^4$  periods starting from a fully mixed configuration. Particles colored in green (light gray) are of species  $A$  while particles colored in red (dark gray) are of species  $B$ . Symbols in the left upper corner correspond to symbols used in (e). In (a) the coordinate frame is shown and the direction of the driving field is indicated by the broken arrow. In (a)–(d) the length of the solid bars (bottom left corner) correspond to the amplitude of a free particle driven without noise in the external field. For small  $Pe$ , we observe a disordered state (a), for intermediate  $Pe$  colloids segregate into stripes oriented perpendicular or tilted (tilt angle  $\theta$ ) to the direction of the oscillating force [(b)–(c)], on the other hand, for high  $Pe$ , lanes are formed parallel to the direction of the oscillatory force (d). Parameters are  $\omega\tau_D=4$  and  $Pe=2, 10, 20, 110$  from (a) to (d). (e) Nonequilibrium steady-state phase diagram for fixed area fraction  $\phi=0.4$ . The solid line describes the simple theoretical estimate of the disordered-to-segregated phase boundary.

$v_d/\omega$  is indicated as an inset in the corresponding simulation snapshots in Figs. 1(a)–1(d). At high frequencies, an ensemble of many particles is just rattling over a small distance and is thus not perturbing much the disordered equilibrium

state. Conversely, at very low frequencies and at a critical  $Pe$ , *lane formation* similar to that observed earlier for a static or slowly oscillating drive [9] occurs where the direction of the lanes coincides with the drive direction. A corresponding simulation snapshot is given in Fig. 1(d). In a region of finite frequencies and Peclet numbers, bounded by disordered and laned steady states, *axial segregation* shows up, where the stripes are oriented perpendicular to the drive direction, see the corresponding snapshot in Fig. 1(b). Here the particles driven alike perform collectively oscillations as induced by the external drive but collide periodically with an opposing band of opposite particles. In Fig. 1(b), a colliding interface is seen in the middle of the snapshot while voids in the two other interfaces indicate that the bands had just been driven away from this position [20]. We call this stripe formation perpendicular to the driving field *axial segregation*. Finally, in a subregion of axial segregation, some steady states are observed with *tilted bands*, see, e.g., the snapshot in Fig. 1(c), where a general tilt angle  $\theta$  relative to the drive direction is observed. However, as discussed in detail below, the major part of the steady states are still segregated in this subregion.

There are two *reentrant effects* of the disordered phase in the phase diagram shown in Fig. 1(e). First by increasing the Peclet number at fixed frequency  $\omega\tau_D \approx 1$ , the steady state transforms from the disordered one into the axially segregated one and back to the disordered one. Second, now for increasing frequency at fixed Peclet number  $5 < Pe < 10$ , the disordered phase is taken over by the axially segregated phase and then appears again.

A simple quantitative criterion for the disordered-to-segregated transition at high frequencies can be derived by the intuitive argument that the oscillating amplitude  $v_d/\omega$  must exceed the mean interparticle distance  $\sigma[\sqrt{\pi/(4\phi_{\text{eff}})} - 1]$  in order to induce a noticeable segregation effect, where  $\phi_{\text{eff}}$  is the effective area fraction with the effective diameter  $\sigma_{\text{eff}}$  determined by the Barker-Henderson expression [21]. The analytical estimate of this phase boundary line is shown as a solid line in Fig. 1(e) and agrees well with the simulation data at intermediate and high Peclet numbers.

We now turn to the dynamics of how the different steady states are reached after turning on the driving field. For this purpose we stroboscopically determine the location of the colloids after each drive period  $T$  (at a time where all external forces vanish) and calculate the partial static structure factor  $S(\mathbf{k}, t) = 2/N |\sum_{i=1}^{N/2} e^{-i\mathbf{k}\mathbf{r}_i(t)}|^2$  as a function of time  $t \equiv nT$ . Here  $\mathbf{k}$  denote the wave vector and  $\mathbf{r}_i$  where  $i \in \{1, \dots, N/2\}$  denote the positions of all particles of the same species. From the structure factor we get the typical length scale of the system via a first moment defined as

$$\frac{\pi}{l_\alpha(t)} = \frac{\int_{-k_{\text{cut}}}^{k_{\text{cut}}} |k_\alpha| S(\mathbf{e}_\alpha \mathbf{k}, t) dk_\alpha}{\int_{-k_{\text{cut}}}^{k_{\text{cut}}} S(\mathbf{e}_\alpha \mathbf{k}, t) dk_\alpha}, \quad (1)$$

where  $\alpha \in \{x, y\}$  and  $k_{\text{cut}}\sigma = 37 \frac{2\pi\sigma}{L}$ .

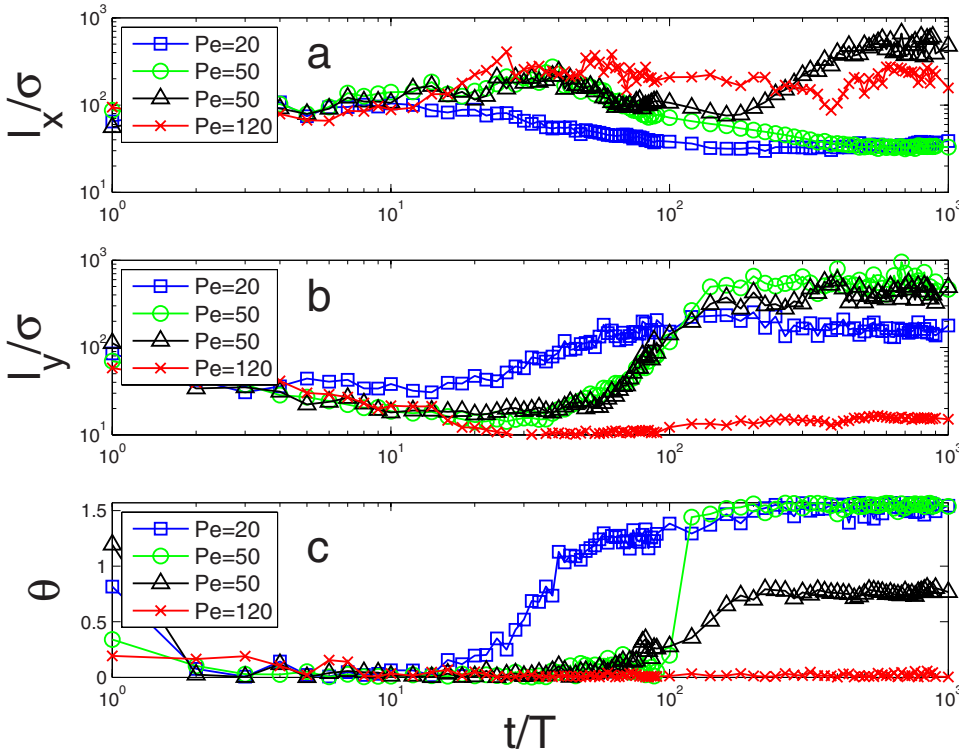


FIG. 2. (Color online) Time evolution of a typical length scale (a)  $l_x/\sigma$  parallel and (b)  $l_y/\sigma$  perpendicular to the direction of the oscillatory force, (c) as well as of the orientation  $\theta$  of a typical structure. The angular frequency is fixed  $\omega\tau_D=4$ . For  $Pe=20$  the system end in an axial segregated state (blue square), for  $Pe=50$  both segregated (green circle) and tilted (black triangle) states occur, whereas for  $Pe=120$  the steady state is laning (red cross).

To obtain the orientation of a typical structure in the system with respect to the direction of the oscillatory force, we calculate the tensor

$$S(t) = \int \int_{-k_{cut}}^{k_{cut}} S(\mathbf{k}, t) [(\mathbf{k}\mathbf{k})\mathbf{I} - \mathbf{k} \otimes \mathbf{k}] d\mathbf{k} \quad (2)$$

(where  $\mathbf{I}$  denotes the unit tensor and  $\otimes$  denotes the dyadic product) and define  $\theta$  as the angle between  $\mathbf{e}_x$  and the eigenvector  $\hat{\mathbf{e}}_1$  corresponding to the biggest eigenvalue of  $\mathbf{S}$ . The angle  $\theta$  serves as an “order parameter” of the observed structures; in fact,  $\theta=0$  points to a state of lanes while  $\theta=\pi/2$  corresponds to axially segregated structures and  $0 < \theta < \pi/2$  indicates a tilted state. Here we choose  $k_{cut}\sigma = 18 \frac{2\pi\sigma}{L}$ .

The time evolution of the two length scales  $l_x$  and  $l_y$  as well as the angle  $\theta$  is shown in Fig. 2 at fixed driving frequency  $\omega\tau_D=4$  for three different Peclet numbers and four different end states, two of which are segregated end state, one is laned, and one is tilted. Strikingly, the system first develops structures along the drive which is persistent over more than a decade in time. It is only after this induction time that the system goes into the final segregated state. This clearly shows that the formation of the axially segregated steady state is a highly collective phenomenon which cannot be accounted for by a local instability analysis. Laning, on the other hand, can be viewed as a local instability [22,23].

Let us now discuss the tilted state, see Fig. 1(c) for a simulation snapshot, in some more detail; in the range  $30 < Pe < 80$  some steady states possess a nontrivial winding around our “toroidal” system (motion in a system with periodic boundary conditions in the  $x$  and  $y$  directions is topologically equivalent to a motion on a three-dimensional toroidal surface), i.e.,  $\theta = \arctan(n/m)$  with natural numbers  $n, m$

and more precisely we observe  $n/m=1/2, 1/1, 2/1$ . We remark that similar steady states were also found in constant driven diffusive lattice gases [1,24] and in binary mixtures which are driven by nonparallel external forces [25]. We observe that with increasing  $Pe$  the probability  $P(\theta)$ , shown in Fig. 3, to end in a tilted steady state with  $\theta=\pi/4$  increases and gets nearly equal to that of an axially segregated ( $\theta=\pi/2$ ) state for  $Pe=60$ . In the range  $50 < Pe < 60$  there exists even a finite probability  $P(\theta)$  for a third steady state

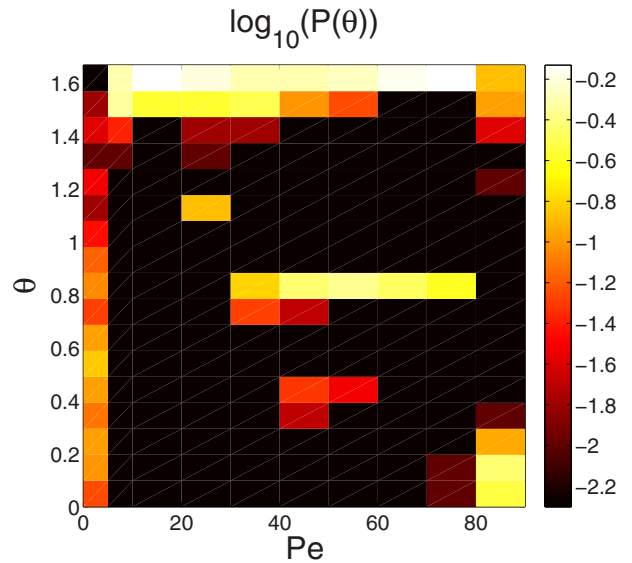


FIG. 3. (Color online) Distribution of the orientation  $\theta$  of the steady-state structures starting from a fully mixed configuration after a simulation time of  $10^4 T$ . For every Peclet number 200 independent simulations have been performed. The angular frequency is fixed to  $\omega\tau_D=4$ .

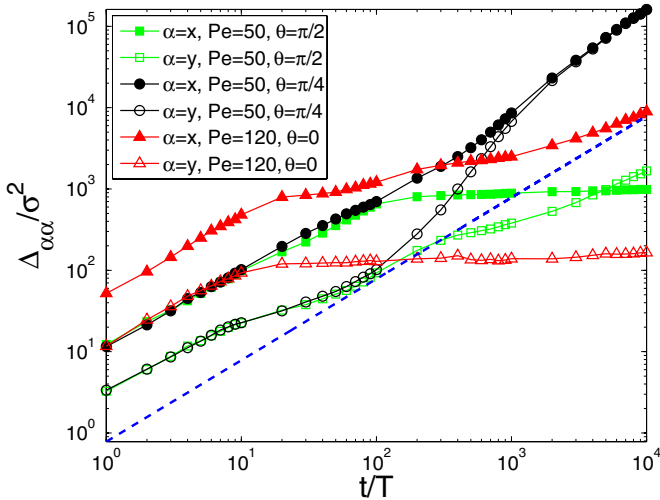


FIG. 4. (Color online) Log-log plot of the mean-square displacement  $\Delta_{xx}$  (filled symbols),  $\Delta_{yy}$  (open symbols) for fixed  $\omega\tau_D=4$ . Green squares and black circles are for  $Pe=50$  and orientations  $\theta = \pi/2$  and  $\theta = \pi/4$ , respectively. Red triangles represent  $\Delta_{\alpha\alpha}$  for  $Pe=120$  and  $\theta=0$ . The long-dashed blue line corresponds to the mean-square displacement of a free colloid.

$\theta = \arctan(2)$ . On average the tilted state is reached after  $10^2 - 10^3$  periods and was always stable during further  $10^5$  periods. We checked that doubling the system size yields again a tilted state with same angle  $\theta$ . Though this clearly shows that tilting is persistent, we cannot exclude at this stage that the tilting is an artificial finite-size effect stemming from the toroidal boundary conditions. However, one can speculate [24] that the lifetime of the tilted states diverges with system size. If so, this would be an example for multistability in a finite region of the  $Pe - \omega\tau_D$  space as a consequence of nonequilibrium dynamics [26].

We finally monitor the mean-square displacement as a function of time  $t$  in the region of multistability and define the corresponding displacement correlations,

$$\Delta_{\alpha\beta}(t) = \frac{1}{N} \sum_{i=1}^N (\Delta \mathbf{r}_i(t) \cdot \mathbf{e}_\alpha) (\Delta \mathbf{r}_i(t) \cdot \mathbf{e}_\beta), \quad (3)$$

where  $\Delta \mathbf{r}_i(t) = \mathbf{r}_i(t) - \mathbf{r}_i(0)$  and  $\alpha, \beta \in \{x, y\}$ . More precisely we consider systems which end up in one of the three steady states with  $\theta = 0, \pi/4, \pi/2$ . The two cases  $\pi/4, \pi/2$  are calculated at the same Peclet number  $Pe=50$ . Results for  $\Delta_{\alpha\beta}(t)$  are presented in Fig. 4 on a double-logarithmic scale. We conclude that for small times the motion is diffusive while for long times it is either diffusive or bounded. A quasi-bounded motion arises if the mean-square displacement is taken for motion perpendicular to the structures formed. In comparing the axially segregated state with the tilted state, the mean-square displacement of the two systems is indistinguishable during the first  $10^2$  periods, but enhanced compared to a free colloid due to enormous number of interpar-

ticle collisions which increase the particle mobility. Moreover,  $\Delta_{xx} > \Delta_{yy}$  for small times due to initial local laning. For  $t/T > 10^2$  and  $\theta = \pi/2$ , particles can unhindered diffuse in the  $y$  direction and trapped in the  $x$  direction ( $\Delta_{xx}$  is nearly constant), while for  $\theta = \pi/4$  the particles diffuse equally in the  $x$  and  $y$  directions. Comparable to a finite mass current along the tilted interface in driven lattice gases [24], we notice that for  $\theta = \pi/4$  the off-diagonal part of the MSD does not vanish  $\Delta_{xy} \neq 0$  which is a consequence of a shear-flow-like displacement field. This is opposed to  $\theta = 0, \pi/2$  where  $\Delta_{xy}$  vanishes.

In conclusion, we have shown that two species of oscillatory driven colloids segregate into stripes perpendicular to the drive for appropriate frequencies and driving strengths. We have performed additional simulations which show that axial segregation is stable in various situations: (i) for softer interparticle interactions, (ii) in three spatial dimensions where the stripes are two-dimensional sheets of finite width, (iii) in slit-geometry confinement when the driving is perpendicular or parallel to the slit, (iv) if hydrodynamic interactions mediated by a solvent flow are included in the simulation and the physical volume fraction is small. The disordered state can be reentrant for increasing the driving frequency and strength. For increasing strength there is a transition toward lane formation delineated by a mixed situation of segregation and tilted stripes.

In principle, it is possible to verify the segregation effect in real-space experiments on driven binary colloidal mixtures. Experimental realizations are superparamagnetic colloids driven by a gradient in a magnetic field [27], oppositely charged colloidal mixtures exposed to an alternating electric field [8], colloids driven by gravity [6,27] in a rotating cell or colloidal mixtures driven by dielectrophoretic force in a non-uniform ac electric field [28]. In particular we think that opposite charged colloids in an ac electric field are a very promising realization to see axial segregation [29]. Since hydrodynamic interactions are strongly screened in this case [30], our model suitably generalized to three spatial dimensions and Yukawa pair interactions should be appropriate to describe this system.

It would be interesting to explore higher densities where freezing occurs [25] and to investigate the solvent flow field which might strike back to the pattern formation at intermediate physical volume fractions. Finally, it is challenging to describe axial segregation by a microscopic theory based on the Smoluchowski equation where either dynamical density-functional theories [22,23] or mode-coupling approaches [31] could be used. We leave this important study for the future.

We thank R. Zia, A. van Blaaderen, A. Imhof, P. Royall, M. P. Ciamarra, and T. Vissers for helpful discussions. We acknowledge ZIM Düsseldorf and Jülich Supercomputing Center (SoftComp Cluster) for computing time. This work was supported by the SFB TR6 (DFG) within project D1.

- [1] B. Schmittmann and R. K. P. Zia, in *Phase Transitions and Critical Phenomena*, edited by C. Domb and J. Lebowitz (Academic, London, 1995), Vol. 17.
- [2] I. S. Aranson and L. S. Tsimring, *Rev. Mod. Phys.* **78**, 641 (2006).
- [3] J. M. Ottino and D. V. Khakhar, *Annu. Rev. Fluid Mech.* **32**, 55 (2000).
- [4] H. Löwen, *J. Phys.: Condens. Matter* **13**, R415 (2001).
- [5] K. R. Sütterlin *et al.*, *Phys. Rev. Lett.* **102**, 085003 (2009).
- [6] C. P. Royall, J. Dzubiella, M. Schmidt, and A. van Blaaderen, *Phys. Rev. Lett.* **98**, 188304 (2007).
- [7] T. Okubo, J. Okamoto, and A. Tsuchida, *Colloid Polym. Sci.* **286**, 1123 (2008).
- [8] M. E. Leunissen, C. G. Christova, A.-P. Hynninen, C. P. Royall, A. I. Campbell, A. Imhof, M. Dijkstra, R. van Roij, and A. van Blaaderen, *Nature (London)* **437**, 235 (2005).
- [9] J. Dzubiella, G. P. Hoffmann, and H. Löwen, *Phys. Rev. E* **65**, 021402 (2002).
- [10] Recent investigations with oscillatory drives have revealed quite rich nonequilibrium transitions including, e.g., drive-induced ergodicity breaking, see, e.g., Refs. [32,33].
- [11] T. Mullin, *Phys. Rev. Lett.* **84**, 4741 (2000).
- [12] P. Sánchez, M. R. Swift, and P. J. King, *Phys. Rev. Lett.* **93**, 184302 (2004).
- [13] M. P. Ciamarra, A. Coniglio, and M. Nicodemi, *Phys. Rev. Lett.* **94**, 188001 (2005).
- [14] M. Pica Ciamarra, A. Coniglio, and M. Nicodemi, *Eur. Phys. J. E* **22**, 227 (2007).
- [15] Actually a softened hard-core potential was used,  $V(r_{ij}) = \frac{V_0}{r_{ij}-\sigma} e^{-(r_{ij}-\sigma)/\lambda}$  for  $r_{ij} > \sigma$ , with the interparticle distance  $r_{ij} = |\mathbf{r}_i - \mathbf{r}_j|$ . We fix the interaction strength  $V_0 = k_B T$  and the screening length  $\sigma/\lambda = 20$ .
- [16] D. L. Ermak and H. Buckholz, *J. Comput. Phys.* **35**, 169 (1980).
- [17] M. P. Allen and D. J. Tildesley, *Computer Simulation of Liquids* (Oxford University Press, Oxford, 1991).
- [18] Much smaller area fractions would lead to weakly interacting system where segregation effects are lost. For higher area fractions, crystallization occurs which slows down the segregation effects considerably, see Ref. [13].
- [19] See EPAPS Document No. E-PLLEE8-79-183904 for a movie showing the development from the initial to the steady state. For more information on EPAPS, see <http://www.aip.org/pubservs/epaps.html>.
- [20] An in-depth explanation for the width of the bands and the location of the voids is still needed. For example, Ciamarra *et al.* found for a granular system the width of the bands to increase with increasing oscillation amplitude, see Ref. [13].
- [21] J. A. Barker and D. Henderson, *Rev. Mod. Phys.* **48**, 587 (1976).
- [22] J. Chakrabarti, J. Dzubiella, and H. Löwen, *Europhys. Lett.* **61**, 415 (2003).
- [23] J. Chakrabarti, J. Dzubiella, and H. Löwen, *Phys. Rev. E* **70**, 012401 (2004).
- [24] K. E. Bassler, B. Schmittmann, and R. K. P. Zia, *Europhys. Lett.* **24**, 115 (1993).
- [25] J. Dzubiella and H. Löwen, *J. Phys.: Condens. Matter* **14**, 9383 (2002).
- [26] C. H. Bennett and G. Grinstein, *Phys. Rev. Lett.* **55**, 657 (1985).
- [27] A. Erbe, M. Zientara, L. Baraban, C. Kreidler, and P. Leiderer, *J. Phys.: Condens. Matter* **20**, 404215 (2008).
- [28] J. Zhao, D. Vollmer, H.-J. Butt, and G. K. Auernhammer, *J. Phys.: Condens. Matter* **20**, 404212 (2008).
- [29] The jamming in bands perpendicular to the field discussed in Ref. [8], however, is different from segregation since a dc electric field was applied.
- [30] M. Rex and H. Löwen, *Eur. Phys. J. E* **26**, 143 (2008).
- [31] J. M. Brader, T. Voigtmann, M. E. Cates, and M. Fuchs, *Phys. Rev. Lett.* **98**, 058301 (2007).
- [32] L. Corte, P. M. Chaikin, J. P. Gollub, and D. J. Pine, *Nat. Phys.* **4**, 420 (2008).
- [33] N. Mangan, C. Reichhardt, and C. J. Olson Reichhardt, *Phys. Rev. Lett.* **100**, 187002 (2008).